End-gas auto-ignition of ammonia-air mixture with spark ignition in a rapid compression machine

Ridong Zhang[1], Wei Liu[1], Qihang Zhang[1], Zhi Wang[1*]
[1]State Key Laboratory of Automotive Safety and Energy, Tsinghua University,
Beijing, 100084, China

1 Introduction

Using ammonia as the fuel of internal combustion engines (ICEs) can help realize carbon neutrality thanks to ammonia's carbon-free nature. Moreover, the high research octane number (RON) of ammonia (nearly 130 [1]) makes it an ideal anti-knock fuel for spark-ignition engines. As pointed out by Blarigan et al. [2], engines using ammonia as fuel can operate with higher compression ratios and thus gain higher thermal efficiency. The above benefits make ammonia a promising fuel for ICEs and thus get ammonia more and more attracted. However, related studies [3, 4] have verified ammonia's combustion stiffness, i.e., higher ignition temperature, longer ignition delay time, and lower laminar flame speed when compared with conventional hydrocarbon fuels. Such combustion characteristics might restrict ammonia's mass application in ICEs due to the possible deterioration in engine performance. In summary, using ammonia as engine fuel has both advantages and disadvantages. To more clearly investigate the combustion characteristics of ammonia, the spark-ignition combustion experiments of ammonia were conducted in an optical rapid compression machine with high-resolution pressure acquisition and high-speed photography. Numerical simulations on chemical analysis were also conducted to better understand ammonia's combustion process.

2 Experimental Setup

2.1 Rapid compression machine

Experiments were conducted on the rapid compression machine at Tsinghua University (TU-RCM). Figure 1 shows the schematic of the test section of TU-RCM. A detailed description of the RCM can be found in Ref.[5]. Briefly, the RCM has a combustion chamber diameter of 50.8 mm and a fixed compression stroke of 500 mm. The clearance at the end of compression (EOC) can be adjusted to achieve the target temperature conditions. The compression process takes about 30 ms with half of the pressure increment occurring within 3 ms before the EOC timing (t_{EOC}). Consequently, heat loss and pre-reaction during the compression process can be minimized. Besides, to reduce the temperature inhomogeneity at EOC, a creviced piston is adopted to minimize the vortex rolled up during the compression process [6]. A pair of laser sensors were mounted on the opposite sides of the compression cylinder to detect piston movement and to generate a delayed signal that can trigger the spark plug at

Correspondence to: wangzhi@tsinghua.edu.cn

EOC timing precisely (within 0.1 ms). The spark plug and a pressure transducer (Kistler 6125C) were installed on the edge of the combustion chamber and were used to initiate the combustion process and record the chamber pressure at 100 kHz, respectively. Moreover, a quartz window was mounted on the endcap of the combustion chamber to provide optical access and a high-speed camera (Photron SA-X2) was used to capture the combustion image at a frame rate of 288000 fps.

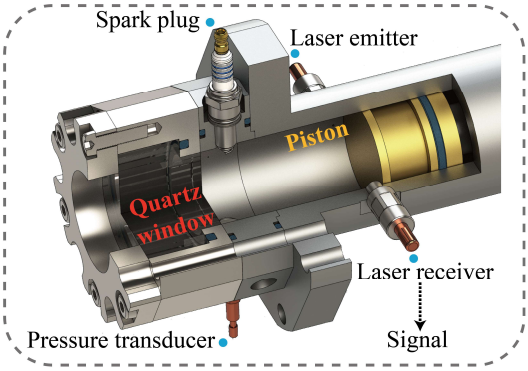

Figure 1 The test section of TU-RCM

2.2 Test conditions

The pressure and temperature at t_{EOC} (denoted as p_{EOC} and T_{EOC} respectively) were used in this study to reflect the thermodynamic conditions. The p_{EOC} was obtained by pressure measurement directly, while the T_{EOC} is calculated from p_{EOC} based on the adiabatic core hypothesis and isentropic correlation that has been widely used for the calculation of temperature in RCM [7], as is shown in Eq.(1),

$$\int_{T_0}^{T_{EOC}} \frac{\gamma(T)}{\gamma(T)-1}\, dlnT = \ln\left(\frac{p_{EOC}}{p_0}\right) \quad (1)$$

where T_0 and p_0 represent the temperature and pressure before compression, and γ represents the specific heat ratio of the mixture.

The experiments were comparatively studied at conditions of T_{EOC} = 730/745/840/925 K, p_{EOC} = 25 bar. The equivalence ratio was fixed at 1 and Table 1 shows the detailed mixture compositions. The test mixtures were composed of NH_3, O_2, N_2, and Ar according to Dalton's partial pressure law and were prepared at room temperature (298.15 K) in a stainless gas tank for at least two hours to ensure homogeneity.

Table 1: Thermodynamic conditions and mixture compositions

p_{EOC}/bar	T_{EOC}/K	φ	NH_3/%	O_2/%	(N_2+Ar)/%
25	730/745/840/925	1	21.88	16.41	61.71

3 Results and Discussions

3.1 Pressure traces

Figure 2 compares the pressure evolution under different temperature conditions. At the condition of p_{EOC} = 25 bar and T_{EOC} = 730 K, the spark ignition fails to initiate the combustion process. The pressure drops gradually after the EOC timing due to heat loss. As the temperature condition rises to T_{EOC} = 745

K, the combustion is successfully initiated and the pressure increases after the EOC timing, reaching a peak value of 62.8 bar. This suggests that the misfire boundary of spark ignition using stoichiometric ammonia-air mixture at p_{EOC} = 25 bar is located within the temperature range of T_{EOC} = 730 ~ 745 K. When the temperature condition was further elevated to T_{EOC} = 925 K, the combustion duration is notably shortened and pressure oscillations with a maximum amplitude of 87.3 bar is observed, implying the occurrence of end-gas auto-ignition. To further interpret the combustion and auto-ignition process, the corresponding image analysis is performed in the next section.

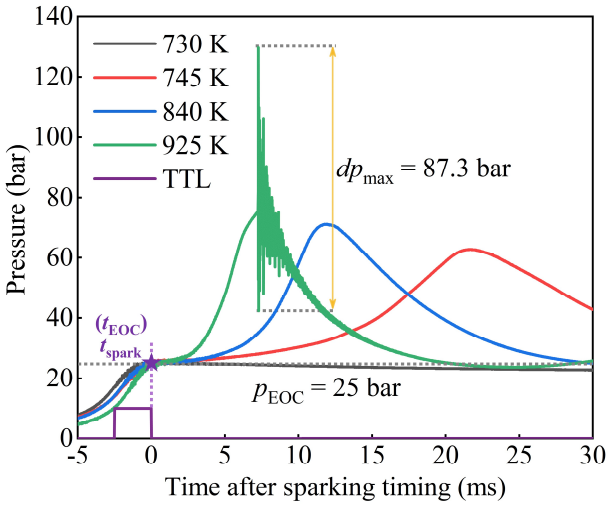

Figure 2 The comparison of pressure traces at p_{EOC} = 25 bar, T_{EOC} = 730/745/840/925 K

3.2 Image analysis

As the visualization results in Figure 3 show, the combustion at T_{EOC} = 745 K and T_{EOC} = 840 K performs similar processes, while that at T_{EOC} = 925 K exhibits different characteristics. Take the conditions of T_{EOC} = 745 K and T_{EOC} = 925 K as examples for analysis. For T_{EOC} = 745 K, the flame initiated by spark ignition propagates at a mean speed of 2.34 m/s during the steady developing stage (marked by Flame1 from t_{spark} to 14.514 ms in Figure 3). Later, at 17.292 ms, the turbulence generated by piston compression that survives near the chamber wall distorts the steady flame propagation and accelerates the local flame, as the Flame2 in Figure 3 shows. In terms of T_{EOC} = 925 K, the steady flame propagation speed averaged from t_{spark} to 3.406 ms increases to 6.50 m/s, and the subsequent local acceleration flame is also observed. Because of the interaction between the steady flame and the acceleration flame, the end-gas is concentrated in the bottom region of the chamber and eventually auto-ignites (abbreviated as A.I. in Figure 3) at 7.208 ms, causing the pressure oscillation on the pressure trace. This suggests that in internal combustion engines fueled with ammonia, knocking combustion may also occur when the temperature at top dead center reaches 925 K, despite ammonia's high RON of nearly 130 [1]. The occurrence of auto-ignition is mainly due to the increasing fuel reactivity and corresponding elevation in chemical oxidation process. To better understand the end-gas auto-ignition that occurred at T_{EOC} = 925 K, the chemical analysis are conducted and the discussions are performed in the following section.

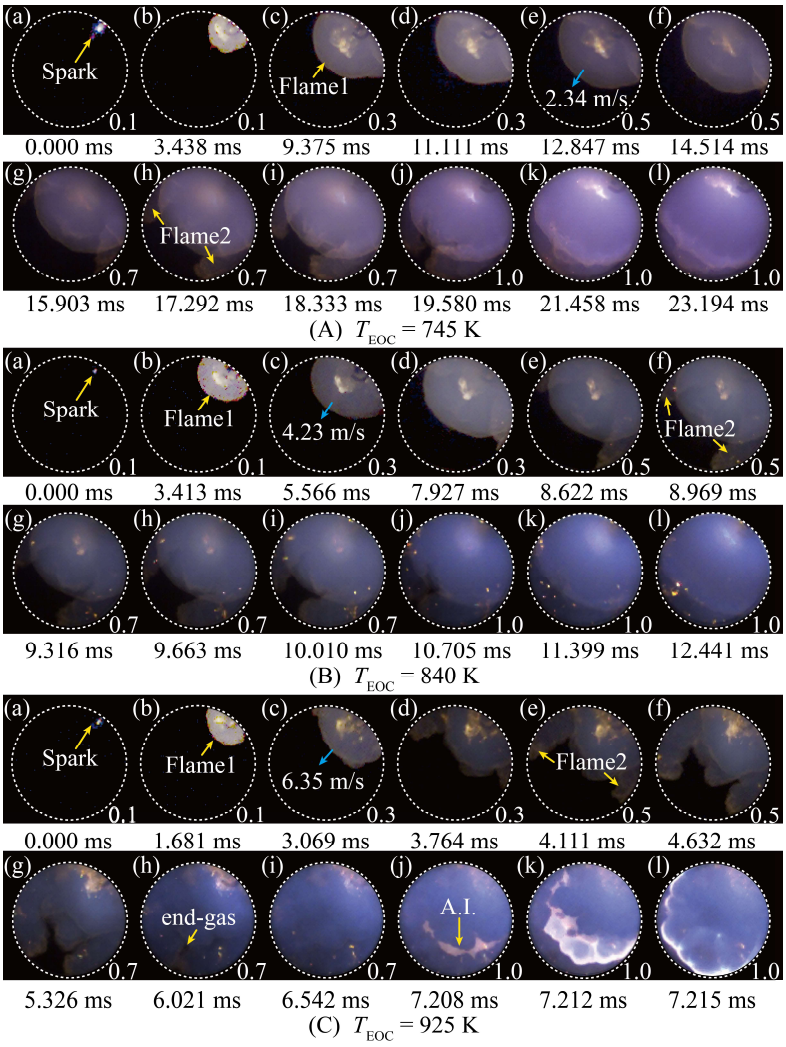

Figure 3 Combustion images at p_{EOC} = 25 bar, T_{EOC} = 745 K/840 K/925 K (Flame1 and Flame 2 represent the steady flame initiated by spark ignition and the acceleration flame induced by turbulence, respectively; the time marked under the images is counted from the t_{spark}; the numbers marked on the bottom right corner of the images are the image gamma values)

3.3 Chemical analysis

In this study, the oxidation process of ammonia-air mixture is simulated using 0-D closed homogeneous batch reactor in Chemkin Pro [8] based on the pressure evolution from t_{spark} to auto-ignition timing. The ammonia oxidation model developed by Liao et al. [9] that has been validated with a fair amount of experimental data was applied in the simulation. For comparison, the experiments under the conditions without and with auto-ignition occurring, i.e., p_{EOC} = 25 bar and T_{EOC} = 745/925 K, were selected to conduct the simulation. Through the simulation, the key reaction pathways (the pathways with a proportion lower than 5 % are not considered) at auto-ignition timing are analyzed. Since there is no auto-ignition occurs at T_{EOC} = 745 K, the pathway analysis is conducted at peak pressure timing instead. The results are summarized in Figure 4. As the results show, NH_3 is mainly consumed through H-atom abstraction reactions including R#1#2#4#5, and produces NH_2 radical. The NH_2 radical can be further converted into other hydronitrogen species, such as N_2H_4, or hydronitrogen oxides, such as H_2NO. At the condition of T_{EOC} = 745 K, the conversions of NH_2 into N_2H_4 and N_2H_3 are dominant. And the

subsequent reactions also mainly involve the hydronitrogen species, i.e., N_2H_4, N_2H_3, N_2H_2, and NNH, as the blue dashed box in Figure 4 signifies. As for the condition of T_{EOC} = 925 K, apart from the reactions among hydronitrogen species, the conversion from NH_2 into H_2NO and the subsequent pathways involve the species of HNOH, H_2NN, HNO, NO, and NO_2 also play important roles in ammonia oxidation, as the red dashed box in Figure 4 signifies. H_2NO is the precursor of HNO and is mainly consumed through the pathways of H_2NO-HNO-NO-NO_2. NO and NO_2 are highly reactive species with strong oxidization, their involvement can significantly enhance the reactive atmosphere. As Figure 5 shows, NO and NO_2 are mainly consumed through the reactions with hydronitrogen species, which accelerates the total oxidation process of NH_3 and promotes the occurence of auto-ignition at T_{EOC} = 925 K.

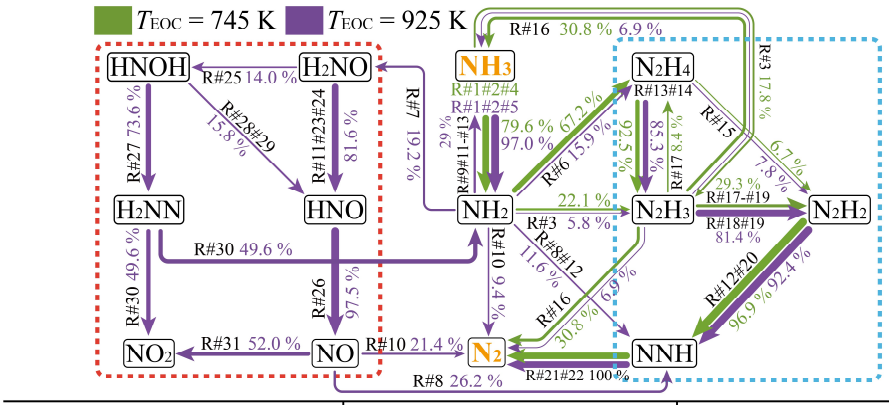

R#1 $NH_3 + OH = NH_2 + H_2O$	R#12 $NH_2 + N_2H_2 = NNH + NH_3$	R#22 $NNH = N_2 + H$
R#2 $NH_3 + HO_2 = NH_2 + H_2O_2$	R#13 $NH_2 + N_2H_4 = N_2H_3 + NH_3$	R#23 $H_2NO + HO_2 = HNO + H_2O_2$
R#3 $NH_3 + NH_2 = N_2H_3 + H_2$	R#14 $N_2H_4 + O_2 = N_2H_3 + HO_2$	R#24 $H_2NO + O_2 = HNO + HO_2$
R#4 $NH_3 + O_2 = NH_2 + HO_2$	R#15 $N_2H_4 = N_2H_2 + H_2$	R#25 $H_2NO + M = HNOH + M$
R#5 $NH_3 + O = NH_2 + OH$	R#16 $N_2H_3 + N_2H_3 = 2NH_3 + N_2$	R#26 $HNO + O_2 = NO + HO_2$
R#6 $NH_2 + NH_2 (+ M) = N_2H_4 (+ M)$	R#17 $N_2H_3 + N_2H_3 = N_2H_2 + N_2H_4$	R#27 $HNOH + NH_2 = H_2NN + H_2O$
R#7 $NH_2 + NO_2 = H_2NO + NO$	R#18 $N_2H_3 + HO_2 = N_2H_2 + H_2O_2$	R#28 $HNOH + HO_2 = HNO + H_2O_2$
R#8 $NH_2 + NO = NNH + OH$	R#19 $N_2H_3 (+ M) = N_2H_2 + H (+ M)$	R#29 $HNOH + NH_2 = HNO + NH_3$
R#9 $NH_2 + HO_2 = NH_3 + O_2$	R#20 $N_2H_2 + HO_2 = NNH + H_2O_2$	R#30 $H_2NN + O_2 = NH_2 + NO_2$
R#10 $NH_2 + NO = N_2 + H_2O$	R#21 $NNH + O_2 = N_2 + HO_2$	R#31 $NO + HO_2 = NO_2 + OH$
R#11 $NH_2 + H_2NO = HNO + NH_3$		

Figure 4 The key reaction pathways of end-gas at auto-ignition timing (p_{EOC} = 25bar, T_{EOC} = 925 K) an d peak pressure timing (p_{EOC} = 25 bar, T_{EOC} = 745 K)

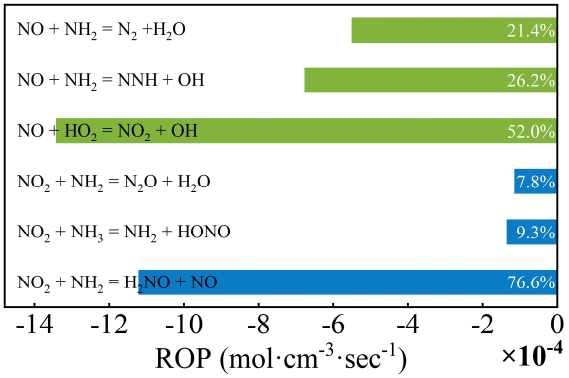

Figure 5 ROP analysis of the consumption reactions of NO and NO_2 at auto-ignition timing under the condition of p_{EOC} = 25 bar, T_{EOC} = 925 K

4 Conclusions

This work investigated the spark-ignition combustion process of ammonia using an optical RCM. The equivalence ratio of the test mixture was fixed as 1, and the experiments were conducted at the

conditions of p_{EOC} = 25 bar, T_{EOC} = 730/745/840/925 K. Through experimental and numerical analysis, the main conclusions can be drawn as follows.

(1) The spark ignition succeeds at T_{EOC} = 745 K but fails at T_{EOC} = 730 K, indicating the misfire boundary of spark ignition using stoichiometric ammonia-air mixture at p_{EOC} = 25 bar is located within the temperature range of T_{EOC} = 730 ~ 745 K.

(2) At the condition of T_{EOC} = 925 K, the auto-ignition takes place in end-gas and causes pressure oscillation with maximum amplitude reaches up to 87.3 bar, indicating the knock tendency of ammonia as engine fuel despite its RON of nearly 130. This also suggests that internal combustion engines using ammonia should not operate under extreme thermodynamic conditions to avoid knocking combustion.

(3) The chemical analysis shows that the reactions among hydronitrogen species are dominant in the oxidation process of ammonia at the condition of p_{EOC} = 25 bar, T_{EOC} = 745 K. When the temperature condition rises to T_{EOC} = 925 K, a fair amount of hydronitrogen oxides, such as H_2NO, and nitrous oxides (NO and NO_2) are produced and play important roles in the oxidation process. The involvements of NO and NO_2 enhance the reactive atmosphere and accelerate ammonia's oxidation process, promoting the occurrence of auto-ignition.

5 Acknowledgment

This study was supported by the National Natural Science Foundation of China (Grant No.: 52076118) and the Joint Research Foundation of Tsinghua and Toyota (Grant No.: 20213930001).

References

[1] A. Valera-Medina, H. Xiao, M. Owen-Jones, W.I.F. David, P.J. Bowen, Ammonia for power, Progress in Energy and Combustion Science 69 (2018) 63-102.
[2] V. Blarigan, Advanced internal combustion engine research, Proceedings of the DOE Hydrogen Program Review, NREL-CP-570-28890, (2000) 1-19.
[3] L. Yu, Y. Mao, Y. Qiu, S. Wang, H. Li, W. Tao, Y. Qian, X. Lu, Experimental and modeling study of the autoignition characteristics of commercial diesel under engine-relevant conditions, Proceedings of the Combustion Institute 37 (2019) 4805-4812.
[4] K.P. Shrestha, C. Lhuillier, A.A. Barbosa, P. Brequigny, F. Contino, C. Mounaïm-Rousselle, L. Seidel, F. Mauss, An experimental and modeling study of ammonia with enriched oxygen content and ammonia/hydrogen laminar flame speed at elevated pressure and temperature, Proceedings of the Combustion Institute 38 (2021) 2163-2174.
[5] H. Di, X. He, P. Zhang, Z. Wang, M.S. Wooldridge, C.K. Law, C. Wang, S. Shuai, J. Wang, Effects of buffer gas composition on low temperature ignition of iso-octane and n-heptane, Combustion and Flame 161 (2014) 2531-2538.
[6] G. Mittal, C.-J. Sung, Aerodynamics inside a rapid compression machine, Combustion and Flame 145 (2006) 160-180.
[7] S.S. Goldsborough, S. Hochgreb, G. Vanhove, M.S. Wooldridge, H.J. Curran, C.-J. Sung, Advances in rapid compression machine studies of low- and intermediate-temperature autoignition phenomena, Progress in Energy and Combustion Science 63 (2017) 1-78.
[8] R. CHEMKIN-PRO, 15083, reaction design, Inc., San Diego, CA, (2011).
[9] W. Liao, Z. Chu, Y. Wang, S. Li, B. Yang, An experimental and modeling study on auto-ignition of ammonia in an RCM with N2O and H2 addition, Proceedings of the Combustion Institute, doi:10.1016/j.proci.2022.07.264(2022).